The International Journal of Pavement Engineering, Vol. 7, No. 1, March 2006, 37–52

Taylor & Francis
Taylor & Francis Group

Mesoscale and microscale evaluation of surface pavement impacts on the urban heat island effects

J. S. GOLDEN†* and K. E. KALOUSH‡¶

†National Center of Excellence on SMART Materials, Global Institute of Sustainability, Arizona State University, P.O. Box 873211, Tempe, AZ 85287 3211, USA
‡Department of Civil and Environmental Engineering, Ira A. Fulton School of Engineering, Arizona State University, P.O. Box 875306, Tempe, AZ 85287 5306, USA

(Received 10 September 2004; revised 7 September 2005; in final form 30 November 2005)

The global phenomenon of rapid urbanization is forcing the transition of native vegetation to man-made engineered surfaces resulting in the urban heat island (UHI) effect. The UHI can adversely impact the sustainability of regions by increasing the dependence of mechanical cooling which results in increased greenhouse gas emissions, consumption of water in the thermoelectric process and increased costs of living for regional residents. The UHI can also increase the incidence and severity of heat related illnesses as well as alter sensitive ecological systems. Mesoscale remote sensing was acquired and reviewed to identify the role of surface pavements on the UHI in the Phoenix region. The imagery provided coarse visual representation of the paved surfaces, including local roads, highways and parking lots pavements; they showed a noteworthy role in regards to the UHI as well as distinguishing variability of surface temperatures related to spatial patterns, pavement material type, location and surrounding landscape. Remote sensing was also used to demonstrate the usefulness of capturing and analyzing surface materials, comparing soil and vegetation indices, *albedo* and surface temperatures. Handheld IR thermography was also utilized in examining contributing factors and mitigation techniques to the UHI. The findings of this study indicated that both mesoscale satellite remote sensing imagery and microscale handheld IR thermography are useful tools for defining and evaluating pavement surfaces temperatures and their contribution to the UHI. However, both have limitations in their use based on the study of interest.

Keywords: Remote sensing; Infrared thermography; Urban heat island; Pavement surface temperatures; Asphalt rubber concrete; Thin whitetopping PCC

1. Introduction

A major influence in the development of the urban heat island (UHI) is the transition of the urban region from native vegetation to that of man-made and engineered materials that have lower *albedo* and greater heat storage capacity (Golden 2004). Various studies have quantified the urban fabric for western urban regions namely through the use of aerial color orthophotography, the global biosphere emissions and interactions system (GLOBEIS) model data and land-use/land-cover (LULC) information from the United States Geological Survey (USGS). Rose *et al.* (2003) identified that paved surfaces cover 29% of the urban fabric, while Akbari *et al.* (1999) reported that 39% of the area seen from above the urban canopy (tree canopy) consisted of paved surfaces, including roads, parking areas and sidewalks. An evaluation of the entire metropolitan areas of Salt Lake City, Utah, Sacramento, California and Chicago, Illinois revealed the percentage of paved areas ranged from 30 to 39% as seen above the canopy, and 36–45% viewed under the canopy layer, primarily due to the absence of rooftops and tree canopies (Gray and Finster 2000, Akbari *et al.* 2001). In residential areas, the paved surfaces were slightly lower at 29–32%.

Because pavements comprise such a significant percentage of the urban fabric, this article expands on prior research and discusses methodologies that were used to examine the impacts of pavements on surface and ambient temperatures. It also examines how pavement designs that utilize recycled waste products may provide

*Corresponding author. Email: jay.goldent@asu.edu. Tel.: + 1-480-965-4951. Fax: + 1-480-965-8087.
¶Email: kaloush@asu.edu

The International Journal of Pavement Engineering
ISSN 1029-8436 print/ISSN 1477-268X online © 2006 Taylor & Francis
http://www.tandf.co.uk/journals
DOI: 10.1080/10298430500505325

an additional sustainable engineering solution to mitigate the microscale impacts of surface temperatures, compared to traditional mitigation methods which alter pavement *albedo*.

Since rapidly urbanizing regions have such a fast rate of change, it is necessary to develop a methodology and a set of tools which allow for the ability to understand the impacts of surface pavement designs as well as mitigation strategies at the same rate of the change. The research conducted in this article utilizes both meso and microscale evaluations of surface pavements through the use of remote sensing, handheld thermography and *in situ* thermocouples.

2. Research approach and methodology

This article is divided into sections that follow a research methodology shown in figure 1. First, mesoscale remote sensing was acquired and reviewed to identify the role of surface pavements and to identify any potential drawbacks in relying solely on satellite imagery as a tool to understand the UHI and mitigation strategies.

Secondly, handheld IR thermography was utilized as a research tool to examine the UHI and the role of surface pavements. Once the capabilities of this research method were compared to mesoscale remote sensing, the next stage of the research was to quantify the accuracy of handheld thermography in comparison to *in situ* thermocouples. Test sections of various common and modified pavement materials/surfaces were utilized for this analysis. The data provided a comparison of the accuracy of handheld thermography and supported research activities with respect to microscale surface temperatures. Additionally, modified pavement materials were also evaluated for their ability to reduce surface temperatures. *In situ* findings were linked backed to mesoscale images to identify any commonalities and how both the meso and microscale research tools can be used in tandem.

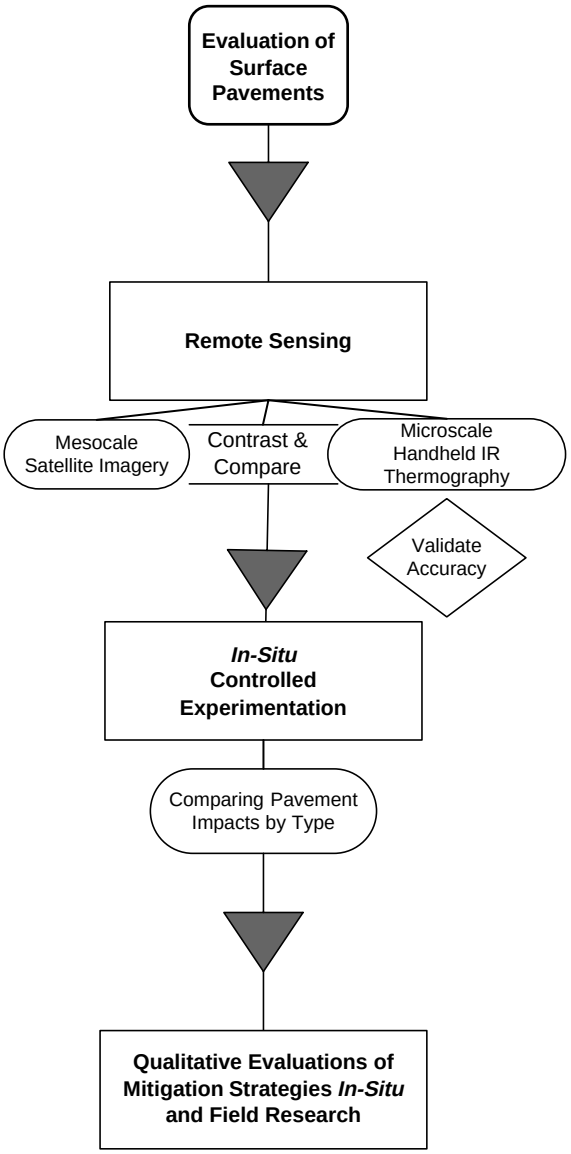

Figure 1. Outline and research scope of work.

3. Mesoscale remote sensing

The first phase of this effort was the acquisition and evaluation of mesoscale remote sensing surface temperature data from the Phoenix region into a visual image as represented in figure 2. The data and processed image was provided from NASA using their advanced spaceborne thermal emission and reflection radiometer (ASTER), which is an imaging instrument that is flying on Terra, a satellite launched in December 1999 as part of NASA's earth observing system (EOS). The ASTER instrument consists of three separate instrument subsystems with spectral ranges and spatial resolutions as shown in table 1. These subsystems are the: visible and near infrared (VNIR), the short-wave infrared (SWIR) and the thermal infrared (TIR).

Satellite sensor data acquisition has been used for evaluating the urban surface temperatures in prior works by Barring *et al.* (1985) and Quattrochi and Ridd (1994).

Table 1. ASTER spectral passband, courtesy of JPL-NASA.

Subsystem	Band number	Spectral range	Spatial resolution (m)
VNIR	1	0.52–0.60	15
	2	0.63–0.69	
	3N	0.78–0.86	
	3B	0.78–0.86	
SWIR	4	1.600–1.700	30
	5	2.145–2.185	
	6	2.185–2.225	
	7	2.235–2.285	
	8	2.295–2.365	
	9	2.360–2.430	
TIR	10	8.125–8.475	90
	11	8.475–8.825	
	12	8.925–9.275	
	13	10.25–10.95	
	14	10.95–11.65	

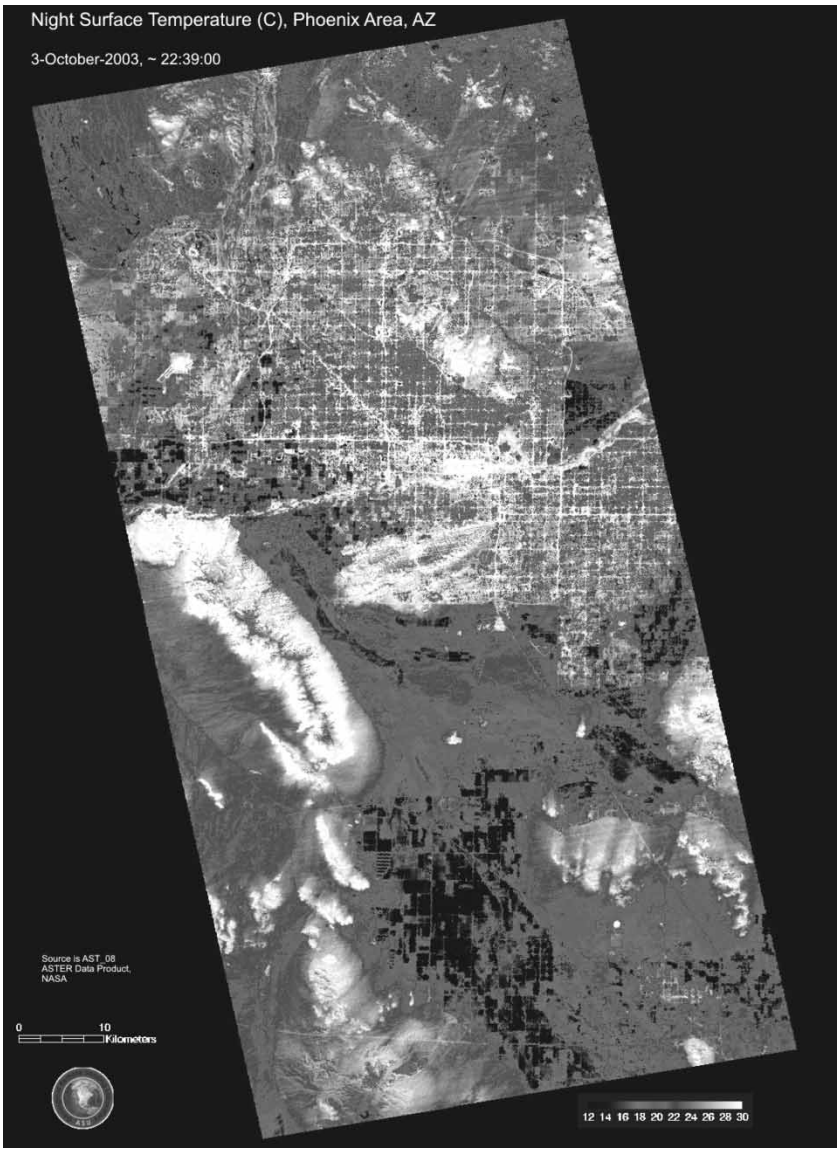

Figure 2. ASTER imagery of surface temperatures for the Phoenix region, 22:39 h on October 3, 2003. Brightest shade of white represents highest surface temperatures. Image provided by NASA-Houston.

As presented in figure 2, ASTER imagery of the Phoenix region captured on 03 October, 2003 at 22:39 h (night time) provided coarse visual representation of the paved surfaces, including local roads, highways and parking lots; they show a significant role in regards to the UHI as well as exhibiting variability of surface temperatures related to spatial patterns and pavement designs.

An image that presents only the surfaces in the top 20% of overall temperatures was processed and is shown in figure 3, where the network of roads and paved surfaces account for a larger percentage by volume of elevated surface temperatures compared to other man-made materials such as residential structures in the region. Of interest in figure 3 are the surface temperatures of the different highway sections in relation to their location. Box A encompasses a section of highway 101 on the east side of Phoenix. The pavement type was a plain portland cement concrete (PCC) for this highway segment at the time the image was taken. It is observed that the pavement surface temperature for the middle section in box A is much less (lighter shade) compared to the top and bottom sections (darker shades) of the same highway segment. The difference was attributed to the grade/elevation of the different segments and the surrounding landscape. The top and bottom sections are depressed or below grade highway segments surrounded by residential areas and sound walls. The surface temperatures of these locations remained higher at night compared to the middle section which was constructed at grade with open landscape fields on the east side.

Another interesting observation is for the highway segment highlighted in box B in figure 3. This is on Interstate 17 that goes north through down town Phoenix. Both the top and bottom segments are below grade with developments and sound walls on either side of the highway. Both sections were built using 30 cm of plain jointed PCC pavement type. The bottom section was overlaid with a 2 cm porous asphalt rubber friction course

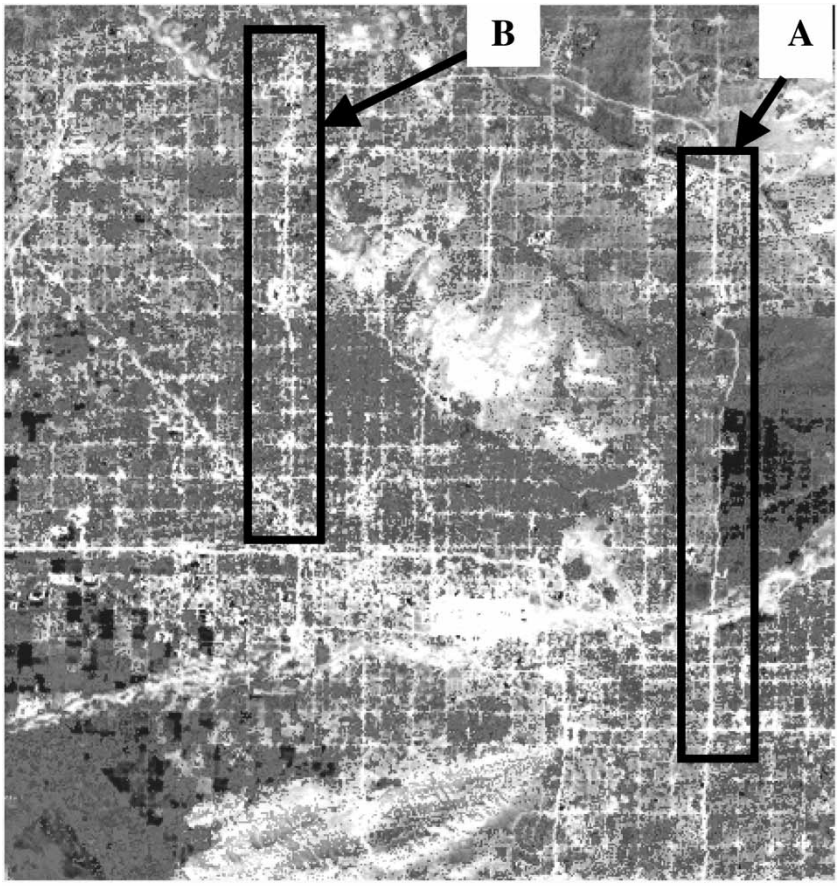

OCT-03 FOR PHOENIX, AZ (1106')

TEMPERATURE

	ACTUAL			NORMAL			
	HI	LO	AVG	HI	LO	AVG	DEPT
1	106	80	93	93	69	81	+12
2	100	80	90	92	69	81	+9
3	96	78	87	92	69	80	+7

Figure 3. ASTER imagery of top 20% of surface temperatures for the Phoenix region, 22:39 h on October 3.

layer; whereas the top portion was left an exposed PCC surface. The blurb in the middle represents metro center, which is a large business and shopping area. From this figure, one can deduce the benefit of using a porous pavement surface layer in reducing the surface pavement temperature at night time as one way to mitigate the UHI.

Mesoscale images such as figure 3 can be utilized as a tool to conduct a preliminary assessment of the impacts of surface engineered materials on a mesoscale resolution and provide for easier identification of the role of surface materials in regards to the UHI. However, the drawback is that these images are merely "snapshots" in time and do not provide for a more detailed analysis of the diurnal temporal cycle. It does, however, provide a benefit by presenting spatial impacts of urban morphology that cannot be viewed except from the satellite. The other limitation is that these images are available only for limited periods of time during the calendar year based on the orbit of the satellite and the priorities of the NASA mission, or priorities of private remote sensing organizations. Furthermore, limitations for researching the influences of pavements and other engineered materials via satellite imagery is that the thermal infrared bands utilized in satellite imagery is limited to 90 m/pixel. For contrast, the visible to near-infrared has a 15 m/pixel resolution which can provide for defining major land cover classes, vegetation health and soil properties. Short-wave infrared has a 30 m/pixel resolution, which can support identification of such things as urban surface materials, ecological communities and fugitive dust emissions. The 90 m/pixel resolution is too coarse to accurately describe what is causing microscale differences of surface temperatures. Beyond the instrumentation limitations, interpretation of the imagery has been shown to present the potential of biases in apparent surface temperatures (Roth *et al.* 1989) due to the effect of the urban surface structure in combination with sun-sensor-surface geometry described as urban surface anisotropy (Voogt and Oke 1997). At a mesoscale level, anisotropy can play a role due to the variations of the geometries of surfaces such as roofs and sides of buildings in comparison to surface parking lots.

Satellite imagery was also used in this study to examine land use change within a region and how it impacted surface temperatures. This experimentation was done for both rural and urban sites. The rural site selected was Gila Bend, Arizona, which is about 120 km southwest of Phoenix.

Remote sensing was used to capture and analyze surface materials, comparing soil and vegetation, *albedo* and surface temperatures as presented in figures 4–9. Daytime data from 19 July 2004 was obtained with the assistance and coordination of researchers from NASA's Mars project who controls data from the Terra satellite.

3.1 Soil and vegetation index

Soil and vegetation index (SAVI) for both urban (Phoenix) and rural (Gila Bend) regions were compared. Figure 4 shows a 30 km transect that was selected from a location of the rural weather station located at Gila Bend Municipal Airport (transect reference 0). The transect direction is to

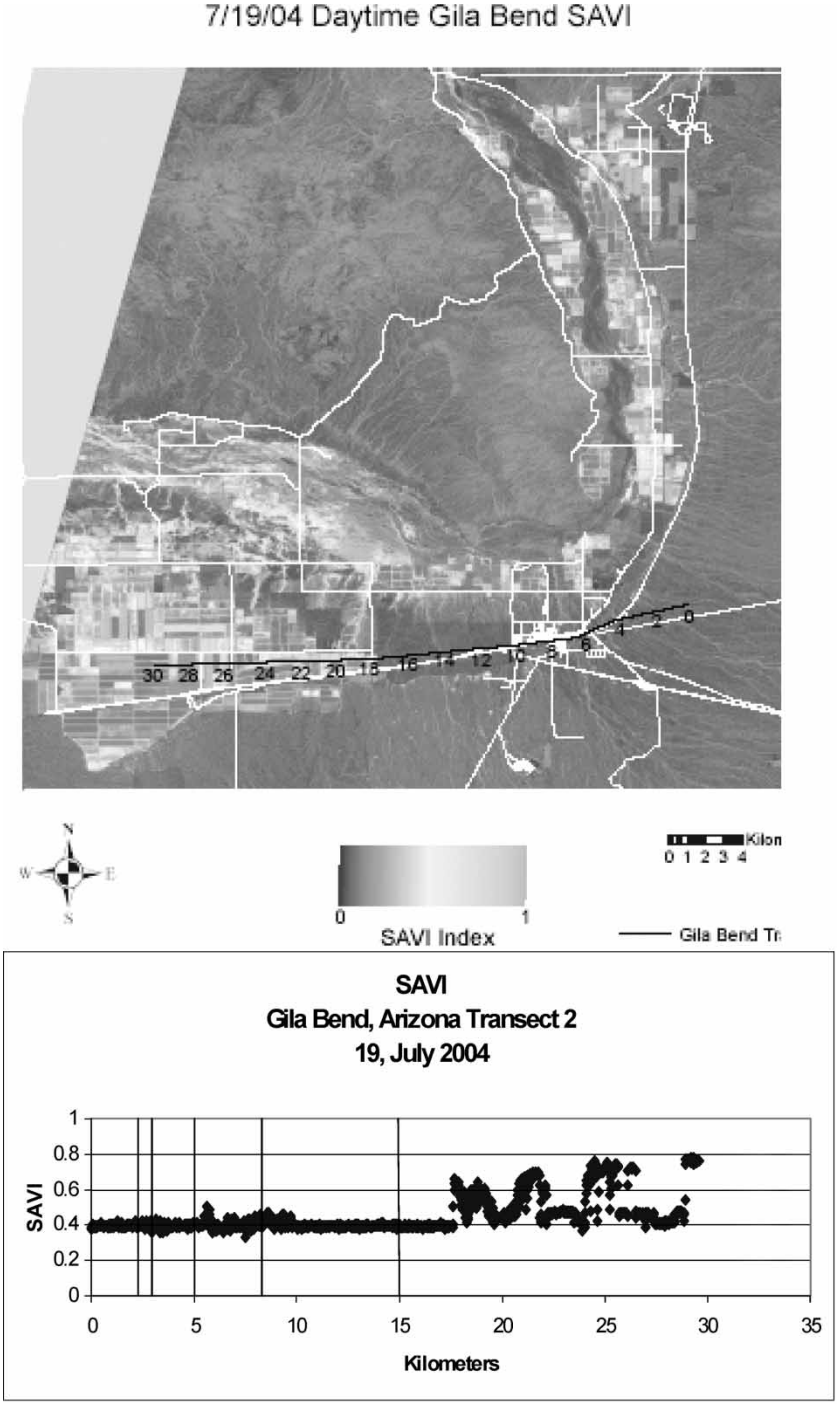

Figure 4. Soil and vegetation index for Gila Bend, Arizona.

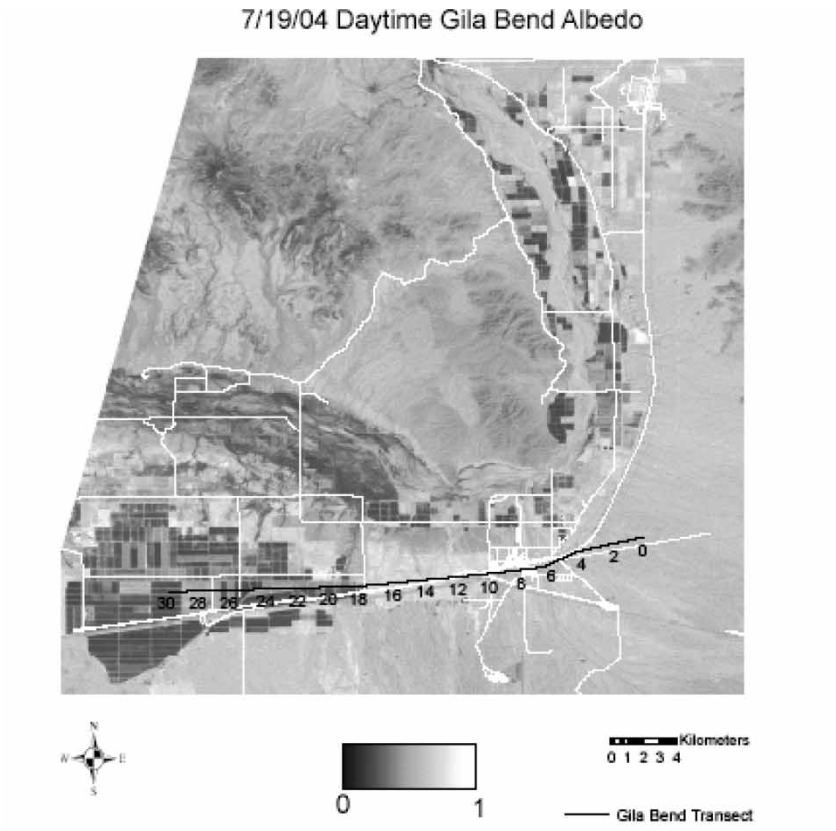

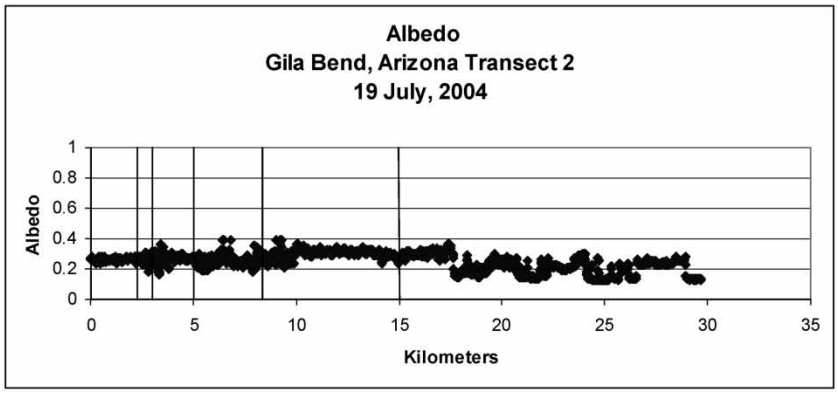

Figure 5. *Albedo* transect for Gila Bend, Arizona.

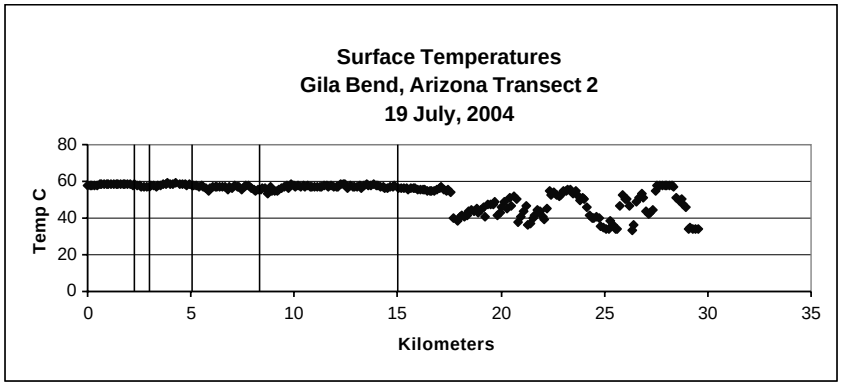

Figure 6. Surface temperatures transect for Gila Bend, Arizona.

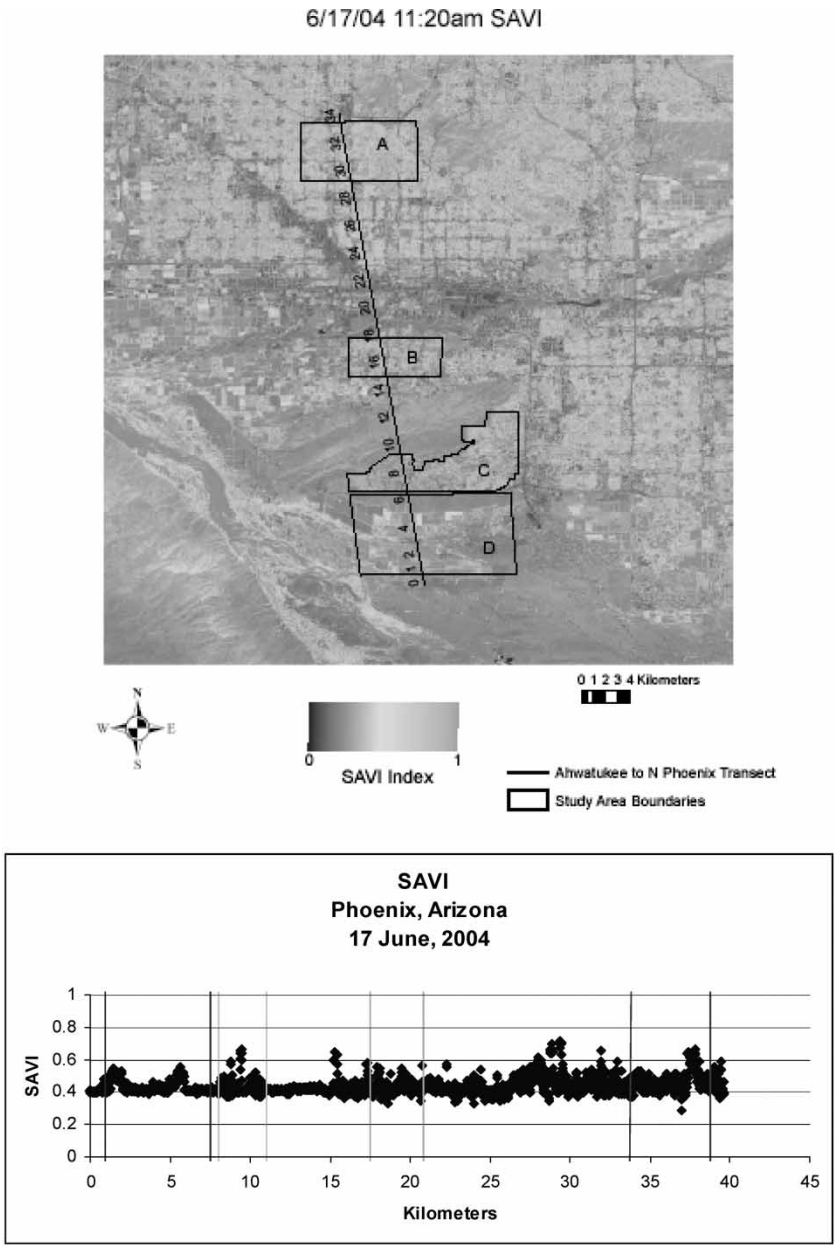

Figure 7. Soil and vegetation index for Phoenix, Arizona region on 17 June, 2004.

the west through the desert (1–6 km), then through a typical rural center city of scattered gas stations and fast food outlets (7–10 km) and ending through agriculture lands (15–30 km). The transect findings indicated that the SAVI index increases as the transect traverses the agricultural lands.

3.2 Albedo

Surface *albedo* measurements for the Gila Bend rural site were obtained for the same date and time using the same transect, as shown in figure 5. The results indicated that areas of higher soil and vegetation indices could have lower *albedo* (but necessarily higher temperature due to evapotranspiration) in comparison to desert landscapes and the small city center portions. The urban portion in this transect is very small and is not representative of an urban core setting.

3.3 Surface temperatures

Surface temperatures from the same image were obtained and placed along the same transect as shown in figure 6. The results indicated that surface temperatures were generally higher where the SAVI was lower.

3.4 Comparison with urban site

SAVI, *albedo* and surface temperatures analysis for a similar transect of the urbanized Phoenix region were also conducted for comparison. This provided a platform to

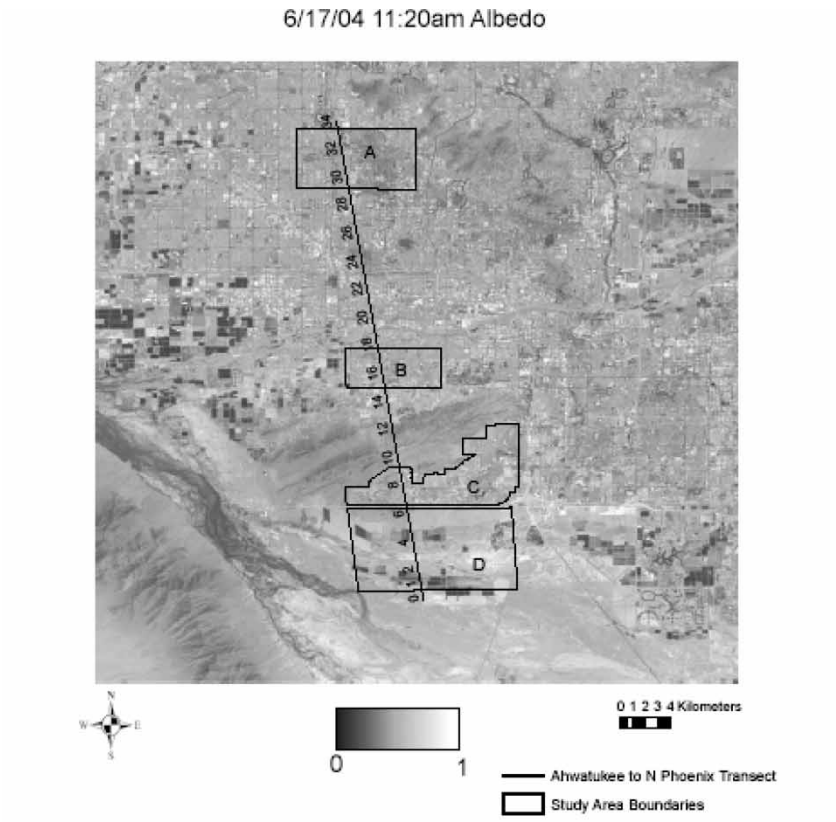

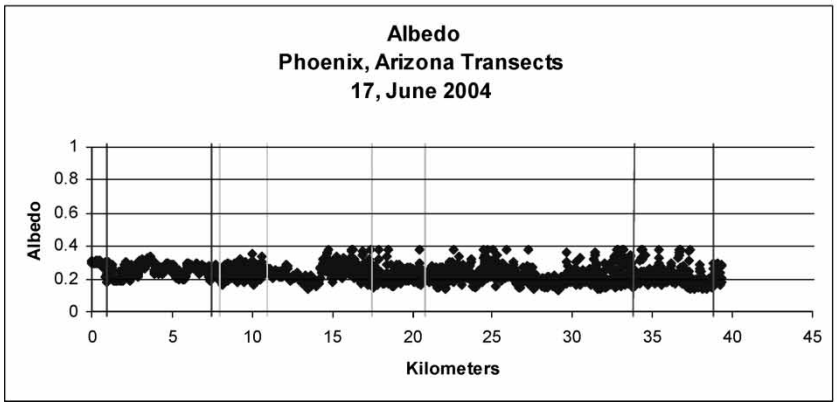

Figure 8. *Albedo* transect for Phoenix, Arizona region on 17 June, 2004.

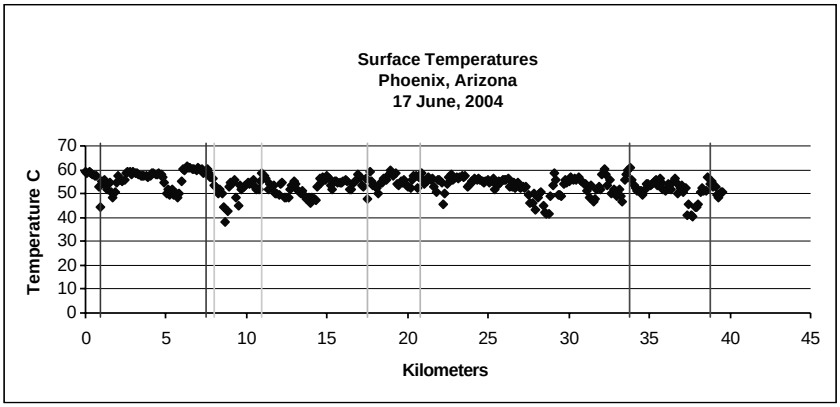

Figure 9. Surface temperatures transect for the Phoenix, Arizona region on 17 June, 2004.

evaluate land use change as a function of urbanization and how it related to ambient air temperature changes over time. The transect conducted for Phoenix is shown as part of figure 7; it began south of the South Mountain Park, a native desert preserve at 0 km, then traveled north through new residential (2–4 km) over the mountain preserve, and then onto the north side of the preserve which has some agriculture (box C) through the downtown core (box B) north through portions of downtown (18–28 km); and finally into an older residential neighborhood with high levels of mesic vegetation (box A).

SAVI results are presented as part of figure 6, whereas, *albedo* results are shown in figure 8 and surface temperatures results are shown in figure 9.

The data presented provided correlations to daytime surface temperatures as a function of *albedo* and SAVI. These data sets were obtained to examine how land use characteristics may contribute to UHI pockets as well as their contribution to the mesoscale UHI. By combining the mesoscale thermal imagery (figure 1) with daytime SAVI and *albedo* transects or histograms, preliminary evaluations can be undertaken to visualize and quantify microscale impacts. Additionally, meteorological equipment can be stationed within areas of research interest, and correlations can be made between surface temperatures obtained from remote sensing in comparison to ambient air temperatures for the same microscale area.

Table 2 presents a comparison of the data collected between the rural and urban areas. This summary data along with images presented earlier (figures 4–9) indicate that the rural area has a higher SAVI and regional *albedo*, and lower surface temperatures. Again, this could be attributed to higher evapotranspiration rates and the lack of complex building morphology in rural areas.

3.5 Benefits and limitations of mesoscale imagery

Clearly, one of the benefits of mesoscale remote sensing as presented in figures 2 and 3, is identifying, spatially, the role of materials contributing to the UHI. Figure 3 presented an image that highways, arterial streets as well as intersections and commercial "strip-malls" and "business offices" parking lots in the Phoenix region have higher surface temperatures compared to other parts of the urban fabric.

Satellite thermal imagery can also be used to identify any areas of the urban region where there are UHI pockets, i.e. concentrations of elevated surface temperatures that also have corresponding elevations in ambient temperatures. Conversely, a mesoscale thermal image can provide visualization of areas that have cooler surfaces compared to other portions of the regions and the associated urban fabric classifications, such as vegetation being the predominant portion of the urban fabric for the cooler pocket. Further analysis of SAVI or *albedo* which was presented in this section can be added to examining cooler or hotter pockets of surfaces in a region.

On the other hand, mesoscale remote sensing has multiple significant impediments to successfully examining the UHI. The image cannot be set NADIR on the area of interest. In addition, the images are obtained at a time convenient for the satellite operator not the researcher, and they cannot be obtained on a continuous basis through the diurnal cycle. Clearly, the images do not also resolve for 3D or complex urban geometry, and resolution are limited to 50 m/pixel.

4. Microscale evaluations

Because of the mesoscale satellite imagery limitations, and in order to gain a better resolution and understanding of the role that surface pavements play within the urban climate, a supplemental research program was developed which included both field investigations throughout the region and the establishment of a controlled outdoor research laboratory. Part of the field campaign was established to quantify and document the use and accuracy of handheld infrared (IR) thermography, and compare it to *in situ* thermocouples for surface temperatures measurements. The goal was to validate the utilization of handheld IR thermography as a tool in examining contributing factors and mitigation techniques to the UHI. The controlled outdoor research laboratory was set up to conduct an examination of seven different pavement designs. The research focused primarily on surface temperatures, as this is the layer that most directly impacts the UHI and is most common in evaluating and comparing the UHI and mitigation strategies. In addition, an on-going effort of this research was the development of a temperature prediction model for a pavement system during a diurnal cycle that accounts for the influence of *albedo* and material's

Table 2. Surface variability analysis.

Land use	Date	Time	SAVI	*Albedo*	Surface temp in (°C)
Urban: Phoenix, Arizona (2,059 *albedo*, 344 surface temperature and 2074 SAVI pixel sets)					
Average	July19, 2004	11:21	0.437	0.233	53.82
Low			0.289	0.134	38.15
High			0.459	0.375	61.25
Rural: Gila Bend, Arizona (1559 *albedo*, 255 surface temperature and 1554 SAVI pixel sets)					
Average	June 17, 2004	11:27	0.457	0.250	52.67
Low			0.334	0.124	33.65
High			0.776	0.375	59.15

thermal and physical properties on the different types of pavements. The model will help in identifying alternative pavement mixes and designs to address the UHI.

4.1 Pavement test sections

The use of an outdoor research facility with experimental pavement test sections was coordinated with the Arizona department of transportation (ADOT) in Phoenix. Figure 10 shows a portion of the layout that was used in this research. Pavement test sections consisted of thick (19 cm) and thin (3 cm) sections of conventional dense graded hot mix asphalt (HMA), an asphalt rubber chip seal surface treatment, thick (19 cm) and thin (3 cm) sections of a gap graded asphalt rubber mixture (typically used in Arizona), thick (30 cm) and thin (10 cm) plain PCC pavement sections, and a plain PCC section modified with 4% by volume using crumb rubber. All of these test sections were constructed per standard ADOT specifications.

4.2 Handheld IR thermography

Handheld IR thermography were conducted to evaluate it as a tool for better understanding the role of surface pavements to the UHI and the effectiveness of mitigation designs. Modern day IR thermography has its roots with Sir Frederick William Herschel, famous for his discovery of the planet Uranus in 1781. Thermography offers a non-invasive analytical method to evaluate thermal characteristics of surfaces within the urban environment. The other benefit of thermography is the ability to obtain almost instantaneous results. Figure 11 shows an example of an image for some surface pavement test sections presented in figure 10. The images are normally provided in color contrast, it was adjusted for gray scale contrast for the purpose of this publication.

The IR thermography unit allows for multiple cross-hair references that capture surface temperatures and emissivity with individual adjustments for ambient temperature, reference temperatures and point of shoot distance. Additionally, manually constructed boxes can be placed within the image to capture the average temperature for the given material or for various cross-hair spots within the box.

During 2003–2004, a campaign was undertaken to examine the urban fabric within the region in different settings. Over 500 initial images were obtained and examined which will eventually lead to a documented library of the diurnal influences of engineered materials in different geo-spatial settings. The campaign included field investigations of highways, arterial streets, parking lots,

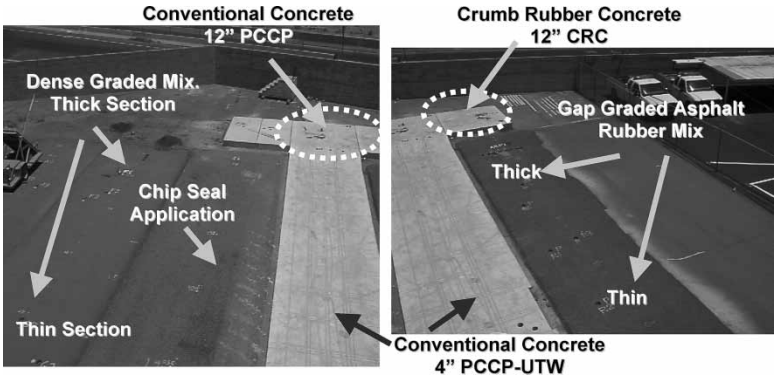

Figure 10. Pavement test sections.

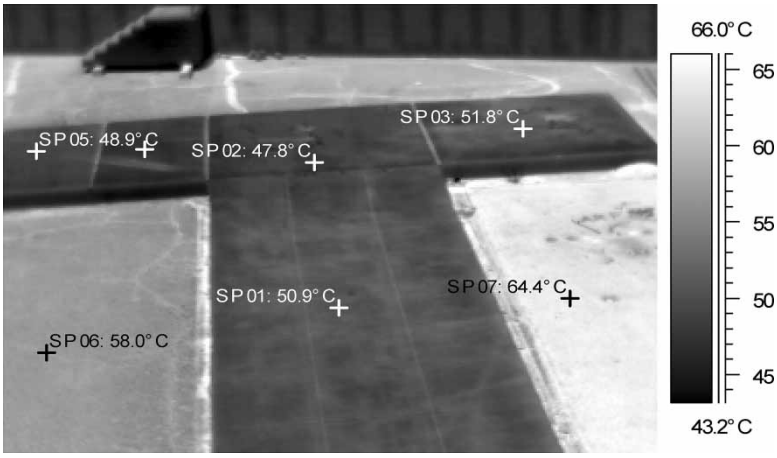

Figure 11. Example of handheld IR thermographic image of pavements.

xeric residential, mesic residential, commercial districts, airports, educational structures and industrial locations throughout the diurnal cycle. Interpretation and visualization of the collected imagery were accomplished with the utilization of software provided by the equipment manufacturer.

Primary field research at the pavement test sections site was conducted in June 2004; June is characterized by calm clear nights and near summer solstice solar alignment. The Phoenix region typically enters the summer monsoon in mid to late July. A FLIR Thermacam™ S-60 IR handheld camera was utilized for this work. The S-60 system consists of an IR camera with a built-in 24° lens, a visual color camera, a laser pointer and a 4″ color LCD on a removable remote control. The unit has a spectral range of 7.5–13 μm with a thermal sensitivity of 0.06° at 30°C and a focal plane of 320 × 240 pixels. The unit is equipped with an internal digital camera that can capture a digital image of the IR subject. Images are stored in either an internal memory or with a memory card.

A 24 h continuous field imaging work, recording surface temperatures every 2 h, were conducted at the pavement test sections. This was done to identify heating and cooling trends (along with data recorded from embedded temperature sensors), verify thermal imagery and thermocouples readings differences (presented later), and identify surface temperature trends for the different paving materials and thickness, if any.

Observations indicated that maximum surface temperature at approximately 1500 h, and a minimum surface temperature between 0500 and 0600 h. The PCC pavements' maximum surface temperature was in the range of 53.5–54.5°C, and the dense graded HMA pavement sections' maximum surface temperature was between 60 and 64°C. Furthermore, the gap graded asphalt rubber mixtures had lower maximum surface temperature (61°C) compared to the conventional dense graded HMA mix (64°C). During the day, the PCC pavements are cooler than the HMA pavements by approximately 6–10°C. There were no significant differences in the low temperatures, and in some cases the PCC pavements were warmer by about 1°C.

Handheld thermography was found to be effective in evaluating homogenous surfaces such as parking lots and also the influences of tree canopy coverage as seen in figure 12. The role of canopy coverage in relationship to surface pavement temperatures is well presented in the use of urban forestry as a mitigation strategy where surface temperatures are seen to be over 20°C cooler under the canopy during midafteroon hours.

Similarly, manufactured canopy coverage benefits in relationship to surface pavements was found to be effectively represented with handheld IR thermography as presented in figure 13 which presents a typical corrugated steel car parking cover in place over a HMA parking lot.

More complex settings with multiple material characteristics require adjusting for various parameters of different influences such as the emissivity for each material. The role of sky view factor and material selection become more important as the urban geometry becomes more complex. For example, sky view factor provides for a faster cooling response of the tile roof in comparison to the sides of the residential building. Although, the tile roof has a lower *albedo* than the white stucco side of the residence, the sides retain a higher surface temperature than the roof. Sidewalks have a similar sky view factor as the roof; however, the thicker mass and heat capacity impacts the retained heat and surface temperature.

Spatial design characteristics also play a role as to how engineered surfaces impact the UHI. Unlike the mesoscale ASTER imagery, handheld IR thermography allows for the acquisition and assimilation of more complex geometries. Anthropogenic heat fluxes are also more identifiable in thermography rather than in satellite imagery. The results of the field campaign provided a platform for the development of a visual library of surface temperatures based on different material types and designs, it also proved to be valuable in quickly acquiring comparative analysis of different surface.

4.3 Validation

The first phase of field validating the use of handheld IR thermography as a tool for evaluating the role of surface pavements was to examine the variability of emissivity. To reduce bias in thermal infrared evaluations the user of handheld thermography must correctly adjust for emissivity, which is defined as the ratio of the emittance of a given surface at a specified wavelength and temperature to the emittance of an ideal blackbody at the same wavelength and temperature. Although, there exists various published listings for the emissivity from vendors, field verification for various materials of concern was undertaken. Several

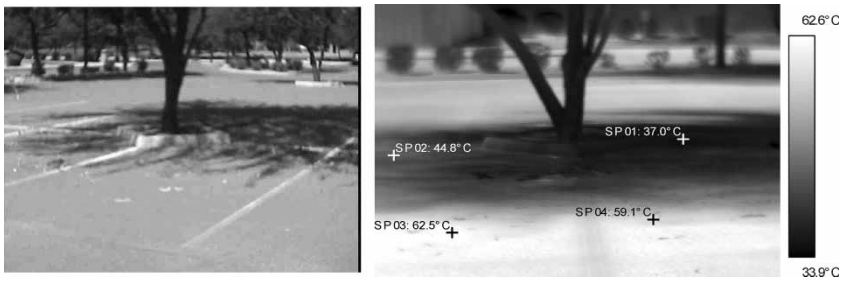

Figure 12. Representation of surface pavement temperatures with urban forestry.

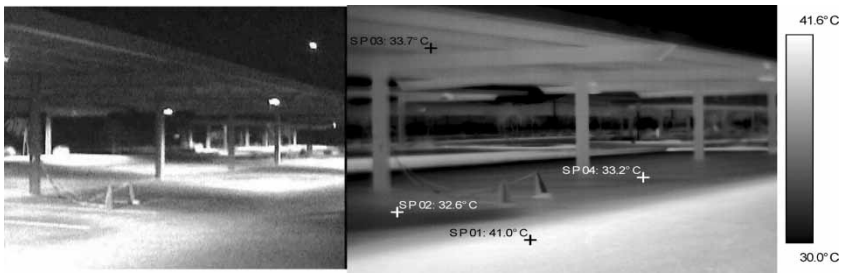

Figure 13. Representation of surface pavement temperatures with engineered canopy coverage.

methods have been developed to calculate the emissivity of different surfaces (Buettner and Kern 1965, Fuchs and Tanner 1966, Idso and Jackson 1968, Zhang *et al.* 1986 and Rubio *et al.* 2003). The method utilized for this research was developed by Reginato of the US Water Conservation Laboratory and described by Fuchs and Tanner (1966).

The equipment utilized was an IR thermometer with a 15° field of view and 8–14 μm band pass inserted into a handmade 63 cm tall aluminum cone (figure 14). The first part of the process was to obtain sky temperature with the IR thermometer connected to a data logger. The cone was pointed skyward at 45° from the horizon and collecting 10 measurements in 10 s as the thermometer was rotated in a circle at orientation. The thermometer was then quickly pointed towards the surface about 1–2 m distant and 5–6 readings were obtained. The cone with the thermometer was quickly placed over the surface of interest and once completely covered the first surface temperature reading was recorded.

A variation of the cone method is the box method. There are two variants of the box method: one lid (Combs *et al.* 1965) and two lids (Buettner and Kern 1965, Rubio *et al.* 2003). At the top and bottom of the box there are two interchangeable lids the "hot lid", which is warmed up, and the "cold lid." Both lids have a small hole through which the radiometer is placed to read the radiance from the bottom of the box. Both methods are effective for horizontal plane emissivity readings in the field with handheld IR thermography. However, this field verification method may not be appropriate when examining complex vertical planes of the urban fabric.

Field trials were conducted to compare the emissivity of common materials in comparison to published results. As presented in table 3, the published results were consistent with this study's field readings.

Figure 14. Cone utilized for field validation of pavement emissivity.

4.4 IR thermography comparison with thermocouples

The next stage of validating handheld IR thermography was to compare the results to *in situ* readings from thermocouples. Thermocouples were utilized to verify the accuracy of hand held thermography as well as to quantify sub-surface temperatures. A field study was set up at the pavements test sections site (previously mentioned) to obtain IR images for approximately a 24 h period on 27–28 June 2004. A mechanical two person lift was used at an elevation of approximately 9 m. The day was characterized as very calm, clear with low humidity and average ambient temperatures. Ambient temperature, humidity, wind direction, rainfall and solar irradiance were collected every 20 min. During the diurnal cycle, maximum wind speeds reached an unsustained 9.7 km/h at 12:00 and 16:00 h with a diurnal average of 3.3 km/h wind

Table 3. Field validation of emissivity.

Material	Published emissivity*	Field trial result
Asphalt paving	0.967–0.970	0.95–0.971
Concrete	0.93–0.97	0.90–0.98
Brick	0.93	0.94

* FLIR systems ThermaCAM 2003.

speed. Humidity reached a maximum of 27% at 09:00 h with and average of 16% relative humidity.

Minimum ambient temperature was 28.33°C at 03:00 on 27 June 2004. That temperature was sustained for 20 min. Maximum temperature reached 39.21°C at 16:20 h on 27 June 2004 and was sustained for 20 min. Sunrise for that date was 05:20 h with sunset at 19:42 h. Solar irradiance as measured in W/m^2 was first recorded at 06:45 on 26 June 2004 at 9 W/m^2, reached a maximum of 945 W/m^2 from 12:20–12:40 h and with a last recorded reading of 4 W/m^2 at 19:45 h.

Table 4 presents the mean temporal difference between the thermal IR imagery to that of the thermocouples for five pavement surfaces. The difference ranged between 0.2 and 5.5°C, with an overall average difference of 0.89°C. Generally, the IR thermography showed higher temperatures than the embedded thermocouples. This was attributed to the difficulties in embedding temperature thermocouples exactly at the surface. The thermocouples utilized in this study were about 0.5 cm thick and were embedded just below the surface. Other contributing factors could have been the various IR angles, placement of the crosshairs on the handheld IR image compared to placement of the thermocouples. In general, trends were consistent between the two methods, except for cases where pavement cleanliness (dust/debris) from patching showed some inconsistencies.

5. Role of *albedo*

As presented earlier, *albedo* is by definition the percentage of absorption of solar energy and thus impacts the temperatures of pavements. Solar radiation includes visible light typically 43% of solar energy, near IR light (52%) and ultraviolet light (5%). *Albedo* will play a role in the day time road surface temperatures as was shown in the previous section. However, *albedo* alone may not be the determinative factor in defining the road surface temperature characteristics through out the full diurnal cycle. Factors such as materials thermal conductivity, heat storage capacity, pavement thickness, density and sky view are all important considerations. This part of the research was considered to understand how *albedo* modifications may impact road surface temperatures extremes in the desert region of Phoenix.

During July 2004, *albedo* alterations were made to the above described pavement test sections. The *albedo* of a road material is the fraction of light incident that is reflected from a surface. Incoming short-wave radiation (K, $\downarrow$ = incoming, $\uparrow$ = reflected) is controlled by the zenith (Z)

Table 4. IR thermography and thermocouple temperatures comparison (°C).

		Dense graded hot mix asphalt			Portland cement concrete (PCC)			Thin whitetopping PCC		
Time	Weather station	Sensor	IR therm	ΔT	Sensor	IR therm	ΔT	Sensor	IR therm	ΔT
12:00	36.56	60.5	58.2	2.3	50.0	50.2	−0.2	50.5	50.3	0.2
13:20	37.44	63.0	62.4	0.6	52.5	51.0	1.5	51.5	51.2	0.3
15:20	38.78	64.0	62.8	1.2	53.5	54.4	−0.9	54.5	55.8	−1.3
17:00	38.89	55.5	56.4	−0.9	49.0	48.2	0.8	51.0	52.3	−1.3
19:00	37.44	44.5	46.2	−1.7	42.5	43.4	−0.9	43.0	45.6	−2.6
21:00	33.17	38.5	44.0	−5.5	37.5	37.3	0.2	37.0	38.0	−1.0
23:00	30.33	35.0	38.2	−3.2	34.5	35.4	−0.9	33.5	32.3	1.2
01:00	28.72	33.0	35.4	−2.4	32.5	33.3	−0.8	31.5	32.0	−0.5
03:00	28.33	31.0	33.3	−2.3	31.0	32.5	−1.5	30.0	31.2	−1.2
05:00	25.94	29.5	31.2	−1.7	30.0	30.3	−0.3	28.5	28.8	−0.3
07:20	27.50	34.0	34.4	−0.4	31.0	32.6	−1.6	31.0	33.0	−2.0
08:40	30.44	41.0	43.0	−2.0	35.5	37.1	−1.6	35.5	36.4	−0.9
			Mean ΔT	−1.45		Mean ΔT	−0.48		Mean ΔT	−0.85

		Crumb rubber portland cement concrete			Gap graded asphalt rubber hma		
Time	Weather station	Sensor	IR therm	ΔT	Sensor	IR therm	ΔT
12:00	36.56	51.0	52	−1.0	55.0	56.4	−1.4
13:20	37.44	53.5	55.6	−2.1	59.0	60.2	−1.2
15:20	38.78	54.5	55.9	−1.4	61.0	63.2	−2.2
17:00	38.89	50.0	51.0	−1.0	58.5	58.8	−0.3
19:00	37.44	43.5	44.2	−0.7	48.5	49.0	−0.5
21:00	33.17	38.0	38.6	−0.6	40.0	39.7	0.3
23:00	30.33	35.0	34.4	0.6	36.0	36.4	−0.4
01:00	28.72	33.0	32.6	0.4	34.0	33.5	0.5
03:00	28.33	31.5	32.4	−0.9	32.0	31.7	0.3
05:00	25.94	30.0	31.2	−1.2	30.5	31.9	−1.4
07:20	27.50	31.0	32.8	−1.8	31.5	32.5	−1.0
08:40	30.44	35.0	36.8	−1.8	37.0	36.7	0.3
			Mean ΔT	−1.05		Mean ΔT	−0.64

Total Mean ΔT −0.89

Table 5. Influence of *albedo* on pavement surfaces, 24 July 2004—Phoenix, Arizona.

Pavement section	$K\downarrow$	$K\uparrow$	α	Surface temperature (°C)
HMA thin	827.3	167.3	0.20	63.3
HMA thin with white paint*	863.2	220.0	0.25	58.3
HMA thick	863.2	146.4	0.17	62.8
HMA thick with white paint*	863.2	221.4	0.26	56.1
Chip seal	863.1	130.2	0.15	62.8
12″ PCC	827.1	376.7	0.46	51.1
Crumb rubber PCC	845.1	356.3	0.42	53.9
Asphalt rubber thick	844.8	111.7	0.13	66.7
Asphalt rubber thick with white paint*	862.8	223.3	0.26	51.1
Thin PCC	862.8	369.5	0.43	53.9
Asphalt rubber thin	862.8	106.4	0.12	67.2
Asphalt rubber thin with white paint*	844.8	105.5	0.12	65.0

* Light application of commercial white paint.

angle of the sun relative to the horizon, with a maximum at the local solar noon (Oke 1987). *Albedo* (α) is not a perfect constant throughout the day, however, $K\uparrow$ can be expected to be reduced in proportion to $K\downarrow$ since the surface is not opaque to short-wave radiation ($\psi_{\text{short}} = 0$). Therefore, the percent of $K\downarrow$ that is not reflected is absorbed, which can be represented as:

$$K^* = K\downarrow - K\uparrow \quad = K\downarrow(1-\alpha) \tag{1}$$

A field survey of each pavement material was conducted on a calm, clear day to determine *albedo*. A pyranometer was used to measure the intensity of the solar radiation by converting light into a dc voltage, which was fed into a voltmeter and data logger. Bolz and Tuve (1973) documented HMA pavement *albedos* from 0.05 to 0.15 with aging as a factor.

Table 5 summarizes the *albedo* measurement for pavements test section for this study. The table also includes results from modifying *albedos* through the use of light application of commercial white paint on some of the test sections. The results show the expected trends of surface temperature reduction with increased *albedo* values.

Prior works in *albedo* modification research is typically focused primarily on reducing surface temperatures of conventional pavements. This experimentation sought to examine the coupled effect of *albedo* modification in conjunction with pavements that have different designs or modified/unconventional. These non-conventional pavements have different heat capacity, thermal conductivity and porosity. These factors in conjunction with modified *albedo* may provide additional insights to mitigating pavement contributions to the UHI. Consumer spray application white paint was applied in an approximate $1.5\,\text{m} \times 1.5\,\text{m}^2$ centered in all the flexible HMA pavement test sections, and the *albedo* measurements were taken as shown in figure 15.

The results of these measurements (table 5) showed that the gap graded asphalt rubber concrete-thin section had the lowest *albedo* (0.12) as well as the highest peak surface temperature of 67°C. This is compared to the PCC test section which had the highest *albedo* of 0.46 and a surface temperature of 51°C. The difference in the peak temperature is 16°C. The dependence of the change in temperature on the change in *albedo* was: $\Delta T_s/\Delta\acute{\alpha} = (-4.7°\text{K}/0.1)$. This is consistent with prior works including those carried out by Lawrence Berkley National Laboratory which resulted in $\Delta T/\Delta\acute{\alpha}$ ranges of $-3.9°\text{C}/0.1 - 7°\text{C}/0.1$. Of significance were the findings of the asphalt rubber pavements. As presented in table 5, the surface temperature of the thick asphalt rubber

Figure 15. *Albedo* measurements (left) and the application of light application of commercial white paint ($1.5 \times 1.5\,\text{m}^2$ area shown on the left).

pavement went from having the highest surface temperature of 67°C to the lowest surface temperature for all pavements both flexible and rigid, at 51°C with an *albedo* increase from 0.13 to 0.26.

The dependence of the change in temperature on the change in *albedo* ($\Delta T_s/\Delta\acute{\alpha}$) was 12.3°K/0.1, is far higher than typical *albedo* mitigation rates from prior research on conventional pavements. Additionally, while the surface temperature of the modified gap graded asphalt rubber concrete pavement was the same as the PCC pavement (tied as the overall lowest surface temperatures), the asphalt rubber pavement had a 0.20 darker *albedo* than the conventional concrete. However, the thickness of the asphalt rubber pavement was almost half of the PCC pavement, and its density is also lower. Therefore, the *albedo* alone is not the determinative factor in defining the road surface temperature characteristics. The heat storage capacity and pavement thickness may play a larger role.

6. Concluding remarks

Mesoscale remote sensing was acquired and reviewed to identify the role of surface pavements on the UHI in the Phoenix region. The ASTER imagery provided coarse visual representation of the paved surfaces, including local roads, highways and parking lots pavements; they showed a noteworthy role in regards to the UHI as well as distinguishing variability of surface temperatures related to spatial patterns, pavement material type, location and surrounding landscape. Remote sensing was also used to demonstrate the usefulness of capturing and analyzing surface materials, comparing soil and vegetation indices, *albedo* and surface temperatures.

Handheld IR thermography was also utilized as a tool in examining contributing factors and mitigation techniques to the UHI. IR images collected over time can eventually lead to a documented library of the diurnal influences of engineered materials in different geo-spatial settings. A controlled outdoor test site was set up to conduct an examination of several different pavement designs. A 24 h continuous field imaging work was conducted to identify heating and cooling surface temperature trends for the different paving materials. Handheld thermography was found to be effective in evaluating the different pavement designs and also the influences of tree canopy coverage.

Another part of the research was considered to understand how *albedo* modifications may impact road surface temperatures extremes in the desert region of Phoenix. Of significance, the dependence of the change in temperature on the change in *albedo* for the asphalt rubber mixture was far higher than typical *albedo* mitigation rates from prior research on conventional pavements. The *albedo* alone was found not to be the determinative factor in defining the road surface temperature characteristics. The heat storage capacity and pavement thickness were hypothesized to play a larger role.

The findings of this study indicated that both mesoscale satellite remote sensing imagery and microscale handheld IR thermography are useful tools for defining and evaluating pavement surfaces' temperatures and their contribution to the UHI. However, both have limitations in their use based on the study needs.

Satellite imagery is but a snapshot in time and there are currently no satellites dedicated solely to an urban research agenda, which means that reliable and pre-planned imagery of a diurnal cycle is not possible for a specific location. Researchers should develop a more compelling case to bring before funding agencies such as NASA for the development and deployment of an urban research satellite. Thermography is perhaps the only near term instrument which can be used to characterize diurnal surface temperature patterns. Both techniques indicated is that the role of pavements plays an important role in the UHI and further research of surface pavements is necessary to develop appropriate mitigation strategies.

Acknowledgements

The authors would like to thank the joint US EPA-ASU National Center of Excellence for SMART Materials, The American Concrete Pavement Association, Rubber Pavements Association, CEMEX USA, the Arizona Cement Association, the National Asphalt Pavement Association, Ms Lela Prashad of the National Center of Excellence for SMART Materials at Arizona State University, and Dr William Stefanov of the Image Science and Analysis Laboratory, Lyndon B. Johnson Space Center, for their assistance in the development of satellite imagery; Mr Mark Belshe, Capt. Ryan Novotny, and Lt. Keith Centner, for their valuable assistance in the field instrumentation and data acquisition. The authors would also like to acknowledge the Arizona Department of Transportation for their assistance with the pavement test sections.

References

Akbari, H., Pomerantz, M. and Taha, H., Cool surfaces and shade trees to reduce energy use and improve air quality in urban areas. *Solar Energy*, 2001, **70**(3), 295–310.

Akbari, H., Rose, L. and Taha, H., Characterizing the fabric of the urban environment: a case study of Sacramento, California, Lawrence Berkeley National Laboratory, US Department of Energy. LBNL-44688, 1999.

Barring, L., Mattson, J. and Lindqvist, S., Canyon geometry, street temperatures and urban heat island in Malmo, Sweden. *J. Climatol.*, 1985, **5**, 433–444.

Bolz, R. and Tuve, G. (Eds.) *CRC Handbook of Tables for Applied Engineering Science*, 2nd ed., 1973 (CRC: Boca Raton, FL).

Buettner, K. and Kern, D., The determination of infrared emissivities of terrestrial surfaces. *J. Geophys. Res.*, 1965, **70**, 1329–1337.

Combs, A.C., Weickmann, H.K., Mader, C. and Tebo, A., Application of infrared radiometers to meteorology. *J. Appl. Meteor.*, 1965, **4**, 253–262.

Fuchs, M. and Tanner, C., Infrared thermometry of vegetation. *Agron J.*, 1966, **58**, 597–601.

Golden, J.S., The built environment induced urban heat island effect in rapidly urbanizing arid regions—a sustainable urban engineering complexity. *Environ. Sci. J. Integr. Environ. Res.*, 2004, **1**(4), 321–349, 2003–2004.

Gray, K. and Finster, M., *The Urban Heat Island, Photochemical Smog, and Chicago: Local Features of the Problem and Solution*, 2000 (Department of Civil Engineering Northwestern University: Evanston, IL), submitted to Atmospheric Pollution Prevention Division—US Environmental Protection Agency.

Idso, S. and Jackson, R., Significance of fluctuations in sky radiant emittance for infrared thermometry. *Agron. J.*, 1968, **60**, 388–392.

Oke, T.R., *Boundary Layer Climates*, 2nd ed., 1987 (Routledge: London).

Quattrochi, D.A. and Ridd, M.K., Measurement and analysis of thermal energy responses from discrete urban surfaces using remote sensing data. *Int. J. Rem. Sens.*, 1994, **15**(10), 1991–2022.

Rose, S.L., Akbari, H. and Taha, H., *Characterizing the Fabric of Urban Environment: a Case Study of Metropolitan Houston, Texas*, Lawrence Berkeley National Laboratory report LBNL-51448 2003.

Roth, M., Oke, T.R. and Emery, W.J., Satellite-derived urban heat islands from three coastal cities and the utilization of such data in urban climatology. *Int. J. Rem. Sens.*, 1989, **10**, 1699–1720.

Rubio, E., Caselles, V., Coll, C., Valour, E. and Sospedra, F., Thermal-infrared emissivities of natural surfaces: improvements on the experimental set-up and new measurements. *Int. J. Rem. Sens.*, 2003, **24**, 5379–5390.

Voogt, J.A. and Oke, T.R., Complete urban surface temperatures. *J. Appl. Meteor.*, 1997, **36**(9), 1117–1132.

Zhang, C., Zheang, Y. and Klemas, V., Quantitative measurements of ambient radiation, emissivity and truth temperature of a greybody; methods and experimental results. *Appl. Opt.*, 1986, **25**, 3683–3689.